SPE 166434

Breakdown Pressure Determination - A Fracture Mechanics Approach

Xiaochun Jin, Subhash N. Shah, Jean-Claude Roegiers, The University of Oklahoma; and Bing Hou, China University of Petroleum (Beijing)

This paper was prepared for presentation at the SPE Annual Technical Conference and Exhibition held in New Orleans, Louisiana, USA, 30 September–2 October 2013.

Abstract

Accurate determination of breakdown pressure in the presence of pre-existing fracture (e.g., natural fractures or perforations) can assist engineers better manage expected fracture gradients. The classical models by Hubbert and Willis, and Haimson and Fairhurst did not account for the existence of pre-existing fractures in predicting breakdown pressure. In addition, the available fracture models for the calculation of breakdown pressure do not consider nonlinear internal pressure distribution in the pre-existing fracture. Finally, some of them either ignored near wellbore stress concentrations, or they are limited to specific fracture dimensions.

To overcome the limitations of current methodologies, a weight function method is applied to predict breakdown pressure of two general symmetrical radial fractures emanating from a borehole. A weight function parameter table and three weight function parameter correlations are provided for continuous dimensionless crack lengths from 0.001 to 100. For uniform pressure distribution in the pre-existing fracture, the weight function based breakdown pressure is compared against the PSA method [*Paris and Sih*, 1965; *Abou-Sayed et al.,* 1978], the results show a good agreement. Weight functions are applied to predict breakdown pressure for uniform and nonuniform pressure distribution in a pre-existing fracture, and the results prove that the pressure distribution affects the breakdown pressure. Sensitivity studies are conducted to investigate the influence of pre-existing crack length, orientation, in-situ stress contrast, and fracture toughness on breakdown pressure. It indicates that breakdown pressure (1) does not always increase with increasing dimensionless crack length at different stress contrast, and (2) increase with increasing absolute value of deviation angle and fracture toughness. The weight function based breakdown pressure is further verified against measured breakdown pressure from laboratory hydraulic fracturing experiments by fine-tuning fracture toughness. The results are also in good agreement for selected successful fracturing experiments.

***Keywords*:** Hydraulic fracturing; Breakdown pressure; Fracture gradient; Stress intensity factor; Weight function method.

1. Introduction

Fracture-mechanics analysis of the breakdown pressure process is important in both drilling (e.g., leakoff test data interpretation, fracture gradient determination), well construction (e.g., casing design), and hydraulic fracturing (e.g., required

horse power, mini frac analysis) [*Detournay and Carbonell*, 1997]. Leak off testing or extended leak off testing is conducted during drilling and the number of test locations is limited, which restricts the prediction of fracture gradient; significant error can occur if there are pre-existing natural fractures intersecting the wellbore. The expensive Mini Frac test is also conducted at a few targeted formations. Misinterpreting cased hole mini frac test data with continuum mechanics is not uncommon in industry. Having a reliable model for breakdown pressure prediction can help save huge costs of field testing. In fracture mechanics, breakdown pressure is defined as a critical pressure at which fracture occurs at the tip of a pre-existing fracture (e.g., natural fracture intersecting borehole, or perforation emanating from the borehole) [*Ingraffea*, 1977]. In continuum mechanics, it is defined as the critical pressure at which crack occurs during pressurization of a borehole [*Detournay and Carbonell*, 1997]. The peak pressure in the recorded pressure-time curve during Leak off test, Mini Frac, or hydraulic fracturing operation is therefore considered to represent the breakdown pressure. Another important concept is fracture initiation pressure, which is defined as the critical pressure at which a fracture initiates from the position where a perforation intersects the borehole [*Wang and Dusseault*, 1991], or a small initial defect at the wellbore starts to propagate [*Detournay and Carbonell*, 1997]. Fracture initiation pressure is equal to or a little bit lower than breakdown pressure [*Ishijima and Roegiers*, 1983]. Two classical expressions of breakdown pressure have been widely used in the industry for decades:

For impermeable rocks, the Hubert-Willis expression [*Hubbert and Willis*, 1957] is usually selected:

$$P_b = 3\sigma_h - \sigma_H + T - p_o \tag{1}$$

For permeable rocks, the Haimson-Fairhurst expression [*Haimson and Fairhurst*, 1967] is preferred:

$$P_b = \frac{3\sigma_h - \sigma_H + T - 2\eta p_o}{2(1-\eta)} \tag{2}$$

where, P_b is the breakdown pressure, σ_h and σ_H are the minimum and maximum horizontal in-situ stresses, respectively, T is the tensile strength of the rock formation, p_o is the pore pressure, η is the poroelastic parameter in the range of 0 to 0.5 [*Detournay and Cheng*, 1992]. For convenience in this paper, all the input values are positive. In the interpretation of results, the tension is considered as positive, and compression as negative.

The validity and feasibility of Eqs.1 and 2 are based on the assumption that the near wellbore region is intact, homogeneous, and elastic. However, both the formation image logging and core analysis have indicated that natural fractures or mechanically induced fractures near wellbore exist [*Haiqing et al.*, 2004]. The existence of perforations also impairs the authority of Eqs.1 and 2. It has been observed that the influence of initial fracture length on breakdown pressure could not be neglected if it is about 4% of the borehole radius [*Bunger et al.*, 2010]. Therefore, it is important to introduce a reliable fracture mechanics model to calculate this breakdown pressure.

Breakdown pressure has been addressed using fracture mechanics for decades [*Abou-Sayed et al.*, 1978; *Ishijima and Roegiers*, 1983; *Atkinson*, 1987; *Rummel*, 1987; *Rummel and Hansen*, 1989; *Wang and Dusseault*, 1991; *Barry et al.*, 1992; *Weijers et al.*, 1996; *Detournay and Carbonell*, 1997], but few papers covering this topic have been published in the literature, especially in petroleum engineering. An important definition in fracture mechanics is stress intensity factor (*SIF*), which is defined as a parameter predicting the stress state in the vicinity of crack tip caused by a remote loading or residual stress [*Anderson*, 2005]. It is assumed that fracture initiation occurs once the following critical condition is satisfied,

$$K_I = K_{IC} \tag{3}$$

where, K_I is the *SIF* of Mode I fracture (opening mode), K_{IC} is Mode I fracture toughness. Sliding mode fracture is not considered in this paper because shear strength of rock is several times of tensile strength.

A fracture mechanics model has been developed to calculate breakdown pressure for two symmetrical fractures (**Fig. 1**) emanating from the borehole [*Paris and Sih*, 1965; *Abou-Sayed et al.*, 1978; *Barry et al.*, 1992],

$$P_b = \frac{K_{IC} - g(a/R_w)\sqrt{\pi a}(\sigma_H - \sigma_h)Cos2\beta}{\sqrt{\pi a}\, f(a/R_w)} + \sigma_H Cos^2\beta + \sigma_h Sin^2\beta \quad (4)$$

where, a is the pre-existing fracture length, R_w is the borehole radius, f (a/R_w) and g (a/R_w) are calibrated functions listed in **Table 1**.

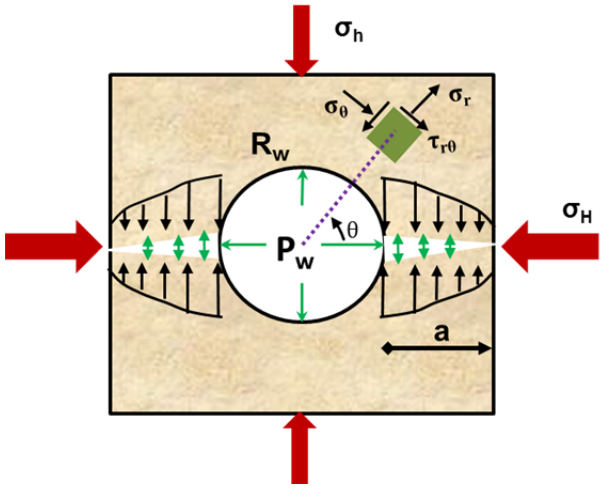

Figure 1 Stress Distribution of Symmetrical Radial Cracks Emanating From the Borehole.

Borehole pressure is represented by $\boldsymbol{P_w}$, while the internal fracture pressure is less or equal to $\boldsymbol{P_w}$. The yellow arrows represent a non-uniform normal stress acting on the crack faces because of near wellbore stress concentrations. The green arrows represent distribution of internal pressure of fracture. $\boldsymbol{\sigma_h}$ and $\boldsymbol{\sigma_H}$ are the two far field stresses. $\boldsymbol{\theta}$ is the angle with respect to maximum horizontal principal stress, counterclockwise direction is positive. $\boldsymbol{R_w}$ is the borehole radius, and $\boldsymbol{a}$ is the crack length.

Because the original fracture model was developed by Paris and Sih, and extended to hydraulic fracturing by Abou-Sayed, Equation 4 is referred to as the **PSA Method** in this paper.

Table 1 Values of $f\,(a/R_w)$ and $g\,(a/R_w)$ for two symmetrical radial cracks
[*Paris and Sih*, 1965; *Barry et al.*, 1992]

a/R_w	$f(a/R_w)$	$g(a/R_w)$	a/R_w	$f(a/R_w)$	$g(a/R_w)$
0	2.26	3.39	1	1.38	1.45
0.1	2.06	2.93	1.5	1.26	1.29
0.2	1.83	2.41	2	1.2	1.21
0.3	1.7	2.15	3	1.13	1.14
0.4	1.61	1.96	5	1.06	1.07
0.5	1.57	1.83	10	1.03	1.03
0.6	1.52	1.71	∞	1.00	1.00
0.8	1.43	1.58			

It is known that the near wellbore stress field is nonlinear because of stress concentrations [*Jaeger and Cook*, 2007; *Fjar et al.*, 2008]. In addition, the internal fracture pressure may not be uniform either. The limitations of current fracture models in hydraulic fracturing are,

(1) Most of the formulas of *SIF* in the handbook are only applicable to uniform and linear loadings [*Tada et al.*, 2000];
(2) Boundary collocation method is employed to calculate the stress intensity factor for two symmetrical radial fractures emanating from a circle, but it is only applicable for fracture aligning with principal stress and not applicable to nonconstant pressure inside the pre-existing fracture [*Newman Jr*, 1971; *Tada et al.*, 2000];
(3) Some models cannot account for nonuniform pressure distribution inside the pre-existing fracture, and only applicable to a specific dimensionless fracture length [*Paris and Sih*, 1965; *Barry et al.*, 1992].
(4) J-integral method is reliable and has been used extensively in fracture mechanics, but is not convenient in engineering practice because of complex numerical integral [*Rice*, 1968b; a].
(5) Technically, SIF can be solved with the weight function method introduced and proved by Bueckner [*Bueckner*, 1970] and Rice [*Rice*, 1972], and developed by Glinka and his group [*Shen and Glinka*, 1991; *Glinka and Shen*, 1991; *Zheng and Glinka*, 1995; *Glinka*, 1996; *Zheng et al.*, 1997; *Kiciak et al.*, 2003]. The weight function for two symmetrical radial cracks emanating from a circle, however, to the best of our knowledge, is not yet available in the literature [*Detournay and Carbonell*, 1997].

The objective of this paper is to integrate the stress concentrations near the borehole with the nonlinear internal pressure in the pre-existing fracture, the dimensionless crack length (ratio of crack length to borehole radius), and the deviation angle between principal stress and pre-existing fracture orientation into one weight function model for the breakdown pressure prediction. Kirsch solutions [*Jaeger and Cook*, 2007], *SIFs* by boundary collocation method [*Newman Jr*, 1971; *Tada et al.*, 2000], and two reference stress intensity factor method [*Shen and Glinka*, 1991] are applied simultaneously in solving for the weight function parameters with numerical programming. A table of weight function parameters for a series of consecutive fracture sizes is provided for the convenience in engineering applications. Three correlation equations of weight function parameters are also derived for scientific computation. Effects of pre-existing fracture orientation and length, in-situ stress contrast, and fracture toughness on breakdown pressure are investigated. Influence of fluid viscosity and flow rate on fluid pressure loss inside pre-existing fracture is not accounted for directly because of the complexity in developing its analytical solution. Instead, a nonlinear equation of pressure inside pre-existing fracture is assumed to study its influence on breakdown pressure. In the sensitivity analyses, breakdown pressure is compared against results attained by the PSA method. Finally, the weight function based breakdown pressure is verified against the measured breakdown pressure in the laboratory hydraulic fracturing experiments.

2. Stress Intensity Factor Derivation Using the Weight Function Method

The weight function is a characteristic property of a specific fracture, and is independent of the applied load [*Bueckner*, 1970; *Rice*, 1972]. It has been widely implemented in engineering fracture mechanics because it simplifies the calculation of *SIFs* under complex loading condition to a relatively simple integration:

$$K_i = \int_0^a \sigma_i(x,\theta) m(x,a) dx \tag{5}$$

$$\text{where, } m(x,a)=\frac{2}{\sqrt{2\pi(a-x)}}\left[1+M_1(1-\frac{x}{a})^{1/2}+M_2(1-\frac{x}{a})+M_3(1-\frac{x}{a})^{3/2}\right] \tag{6}$$

where, i =1, 2, 3; $\sigma_i(x,\theta)$ is the original stress field at the position of pre-existing fracture in an intact rock. It is normal to prospective crack surface. M_1, M_2, and M_3 are weight function parameters. K_i is the *SIF* corresponding to $\sigma_i(x,\theta)$.

The specific problem we are investigating is two symmetrical radial fractures emanating from the borehole, whose 2-D plane strain schematic is as shown in **Fig.** 1. For a specific fracture, its *SIF* under any stress field can be calculated easily after solving its weight function parameters [*Bueckner*, 1970; *Rice*, 1972].

The net stress acting before the fracture is given by:

$$\sigma\left(\sigma_H,\sigma_h,P_w,P(x,P_w),x,\theta\right)=P(x,P_w)-\begin{Bmatrix}-P_w\left(\frac{R_w}{R_w+x}\right)^2+\frac{\sigma_H+\sigma_h}{2}\left[1+\left(1+\frac{R_w}{R_w+x}\right)^2\right]\\-\frac{\sigma_H+\sigma_h}{2}\left[1+3\left(1+\frac{R_w}{R_w+x}\right)^4\right]Cos2\theta\end{Bmatrix} \tag{7}$$

where, x is the distance from wellbore wall, and $P(x, P_w)$ is the internal pressure distribution in the pre-existing fracture.
The major steps of solving weight function parameters are listed in the following:

Step I: Assuming there were no fractures in the body, apply two different stress boundaries, and using Eq. 7 to calculate two different net stress fields σ_1(x) and σ_2(x) on fracture surface.
Step II: Find the corresponding *SIFs* for the two stress fields from the literature, or calculate them via a numerical method if they are unavailable.
Step III: Take the derivative of Eq. 6 with respect to θ at x = 0, and set it equal to zero. This is a geometric characteristic of central and edge cracks [*Fett et al.*, 1987].
Step IV: Solve Eqs. 4-7 simultaneously for weight function parameters.

Following Steps I – III, three formulas were derived for solving the weight function parameters:

$$K_1=\int_0^a\sigma_1(x)\frac{2}{\sqrt{2\pi(a-x)}}\left[1+M_1\left(1-\frac{x}{a}\right)^{1/2}+M_2\left(1-\frac{x}{a}\right)+M_3\left(1-\frac{x}{a}\right)^{3/2}\right]dx \tag{8}$$

$$K_2=\int_0^a\sigma_2(x)\frac{2}{\sqrt{2\pi(a-x)}}\left[1+M_1\left(1-\frac{x}{a}\right)^{1/2}+M_2\left(1-\frac{x}{a}\right)+M_3\left(1-\frac{x}{a}\right)^{3/2}\right]dx \tag{9}$$

$$\text{and, } 1-M_2-2M_3=0 \tag{10}$$

The boundary collocation based *SIFs* [*Newman Jr*, 1971; *Tada et al.*, 2000] for the specific fracture geometry in **Fig. 1** were applied to solve weight function parameters. Details about the derivation and validation of weight function based *SIF* for two symmetrical fractures emanating from circle are published elsewhere [*Jin*, 2013]. A table of weight function parameters is summarized for engineering application in **Appendix**. Three correlations of weight function parameters as shown below are also derived.

$$\begin{aligned}&M_1=0.0356x^5-0.0977x^4-0.1678x^3+0.4661x^2+0.0883x-0.2673\\&R^2=0.9923\end{aligned} \tag{11}$$

$$M_2 = -0.0472x^5 + 0.0735x^4 + 0.2198x^3 - 0.3205x^2 - 0.2037x + 0.1535 \quad R^2 = 0.9959 \tag{12}$$

$$M_3 = -0.0236x^5 + 0.0368x^4 + 0.1099x^3 - 0.1603x^2 - 0.1018x + 0.5768 \quad R^2 = 0.9959 \tag{13}$$

where, $x = Log_{10}(a/R_w)$, $0.001 \le a/R_w \le 100$.

3. Breakdown Pressure Calculation Using Fracture Mechanics

After solving the weight function parameters for different fracture geometries and substituting Eqs. 6 and 7 into Eq. 5, according to fracture initiation criterion in Eq. 3, the following nonlinear equation is obtained,

$$K_{IC} = \int_0^a \sigma(\sigma_H, \sigma_h, P_w, P(x, Pw), x, \theta) \frac{2}{\sqrt{2\pi(a-x)}} \left[1 + M_1\left(1 - \frac{x}{a}\right)^{1/2} + M_2\left(1 - \frac{x}{a}\right) + M_3\left(1 - \frac{x}{a}\right)^{3/2} \right] dx \tag{14}$$

The only unknown is P_w. A numerical program is required to find root of Eq. 14.

4. Sensitivity Study of Breakdown Pressure

In this section, the influence of pre-existing crack length and orientation, fracture toughness, in-situ stress contrast, and internal pressure distribution on breakdown pressure are investigated. When conducting sensitivity studies, the internal pressure distribution of pre-existing fracture was assumed to be constant. Although the flow rate and fluid viscosity affect friction pressure losses in perforations [*Lord and Shah*, 1994], they are not considered in the current research phase. The basic input used in the sensitivity analyses is listed in **Table 2**.

Table 2 Basic Parameters and Their Values for Prediction of Breakdown Pressure

Parameter	Value
Maximum horizontal stress: σ_H	20.0 *MPa*
Minimum horizontal stress: σ_h	15.0 *MPa*
Mode I fracture toughness: K_{IC}	3.0 $MPa \cdot m^{1/2}$
Borehole radius[1]: R_w	0.1 m
Pre-existing crack length: a	Vary
Pre-existing crack orientation: θ	Vary

In this analysis, the breakdown pressure obtaining from the weight function method was also compared against the PSA method. The comparison allows checking for the validity of this approach and identifying its advantages and disadvantages.

4.1 Influence of Pre-existing Crack Length on Breakdown Pressure

The stress concentrations near the borehole vary with distance from the borehole wall. It is difficult to determine the exact penetration depth or natural fracture length intersecting the borehole, although the laboratory testing or logging tools can aid in this estimation. The results are shown in **Fig. 2**.

It can be observed that (1) breakdown pressure decreases with increasing dimensionless crack length for the case currently considered (if the stress contrast is different, the relationship will vary, as is shown later in **Section 4.3**); (2) when

[1] Borehole radius varies with drill bit size. It is assumed as 0.1 *m* in this paper.

dimensionless crack length is less than 0.1, breakdown pressure is very sensitive to dimensionless crack length, and grows exponentially with decreasing dimensionless crack length; (3) Results of both methods agree well with each other; (4) PSA method, however, can only predict breakdown pressure for several specific fracture geometries, which limits its application in the field.

The analysis indicates that for an accurate quantification of breakdown pressure for pre-existing fracture, the knowledge of an accurate fracture length is required, especially for a short fracture.

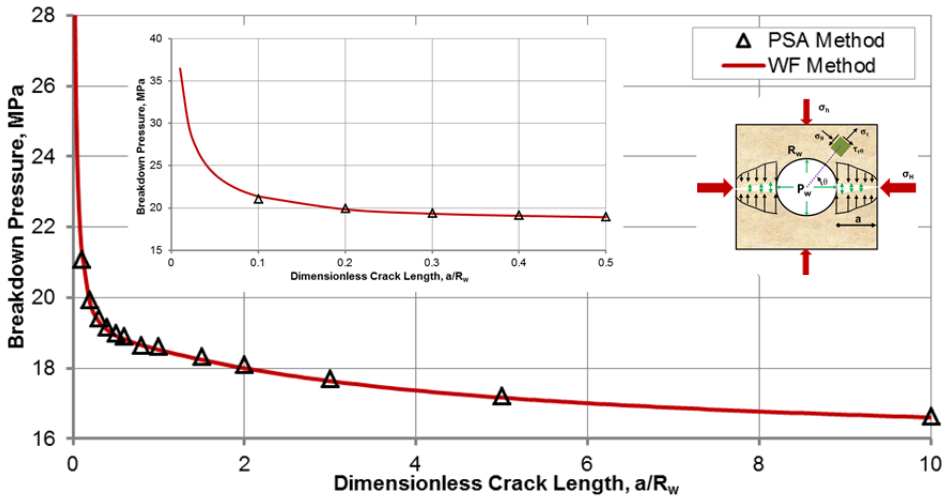

Figure 2 Effect of Dimensionless Crack Length on Breakdown Pressure (R_w = 0.1 m, θ = 0°). The embedded figure is a magnification of breakdown pressure at low dimensionless crack lengths.

4.2 Influence of Crack Orientation on Breakdown Pressure

Perforation guns are recommended to shoot in the maximum principal stress direction to prevent or alleviate fracture tortuosity near the borehole [*Dusterhoft*, 1994; *Yew*, 1997; *Economides and Nolte*, 2000]. In the field, however, it is expensive and difficult to orient the guns to a prescribed direction, and sometimes the information of in-situ stress orientation is not reliable in complex geological environment. In addition, most of the pre-existing natural fractures deviate a few degrees from the maximum horizontal in-situ stress direction [*Higgins*, 2006]. It is known that near wellbore stress varies with the hoop direction [*Fjar et al. 2008*]; consequently *SIFs* of pre-existing fractures at different deviation angle vary.

Keeping other parameters in **Table 2** constant, the results are shown in **Fig. 3**.

It can be observed that (1) breakdown pressure varies with crack deviation angle in a sinusoidal fashion, and increases with increasing deviation angle; (2) Breakdown pressures by both methods agree well with each other for different dimensionless crack lengths. In engineering application, a conservative value of breakdown pressure is suggested and can be calculated by taking an average of breakdown pressures for a series of deviation angles.

4.3 Influence of Stress Contrast on Breakdown Pressure

In-situ stress anisotropy is common in the field [*Jaeger and Cook*, 2007], therefore, studying the influence of stress contrast on breakdown pressure can help engineers foster perception of breakdown pressure in formation with different stress contrasts. Keeping other parameters in **Table 2** constant, investigating the sensitivity of *SIF* of pre-existing fractures to the change of stress contrast by varying maximum horizontal in-situ stress, σ_H = 20, 25, and 30 *MPa*, which corresponds to three

different stress contrasts of 5, 10, 15 *MPa*. The results are shown in **Fig. 4**.

It can be observed that (1) at greater stress contrast, the breakdown pressure does not decrease monotonically with increasing dimensionless crack length at large stress contrasts; (2) there is a minimum value of breakdown pressure near the wellbore (e.g., dotted curve); (3) breakdown pressure by both methods agree well with each other at different stress contrasts. In engineering application, this analysis has proven that it is incorrect to assume that the breakdown pressure for long fracture is lower than for short fracture if the difference in both cases is only the stress contrast.

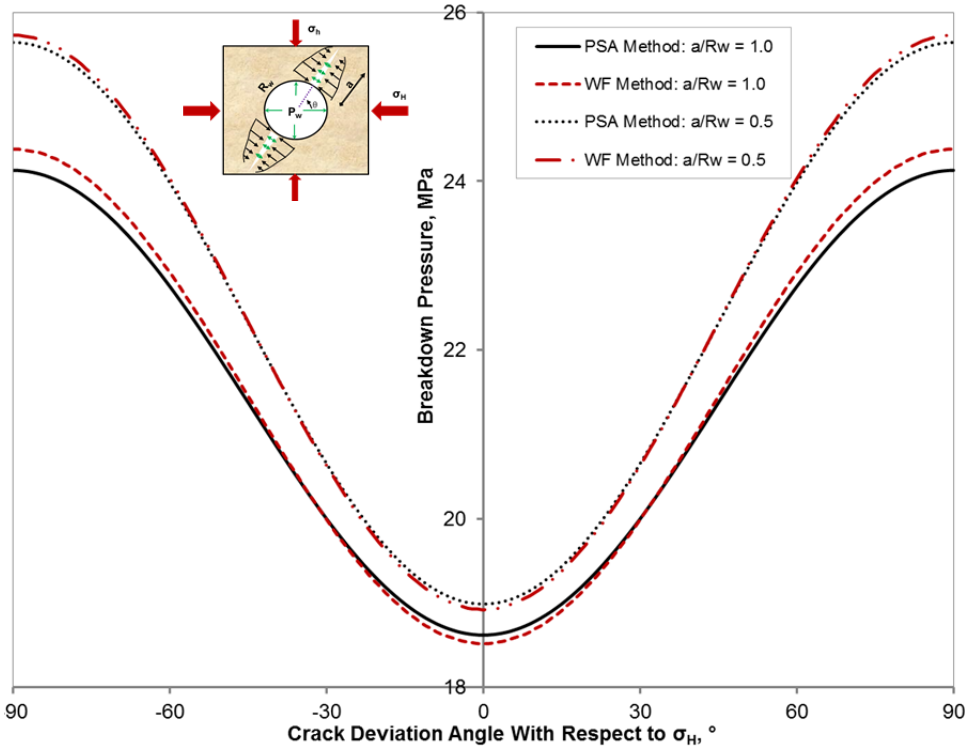

Figure 3 Effect of Crack Deviation Angle on Breakdown Pressure (R_w = 0.1 m)

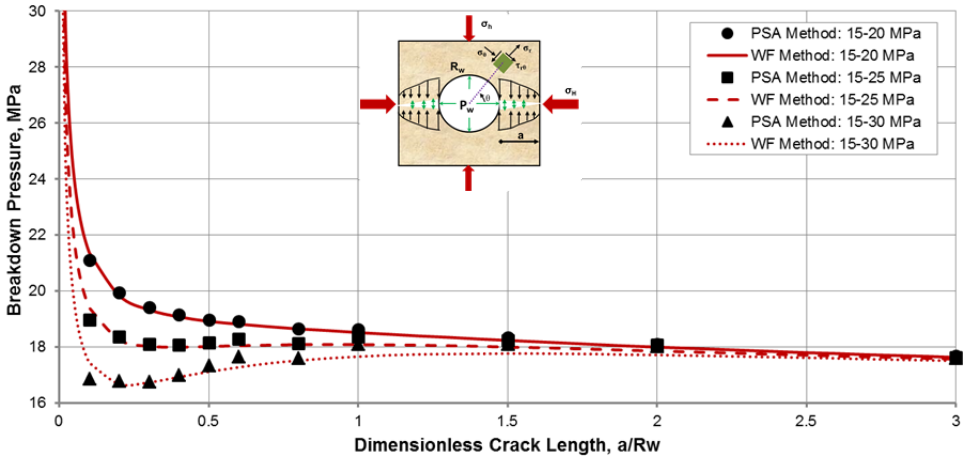

Figure 4 Effect of In-situ Stress Contrast on Breakdown Pressure (R_w = 0.1 m, θ = 0°)

4.4 Influence of Fracture Toughness on Breakdown Pressure

Fracture toughness changes with rock types [*Barry et al.*, 1992]. For the same rock type, increasing temperature or confining pressure will increase the fracture toughness [*Zhao and Roegiers*, 1993; *Al-Shayea et al.*, 2000]. Therefore, the field

measured fracture toughness is usually larger than the laboratory measured fracture toughness [*Shlyapobersky et al.*, 1988]. Keeping other parameters in **Table 2** constant, the effect of *SIF* of pre-existing fractures on fracture toughness is investigated (K_{IC} = 3.0, 4.0, and 5.0 *MPa-m*$^{0.5}$); the results are shown in **Fig. 5**.

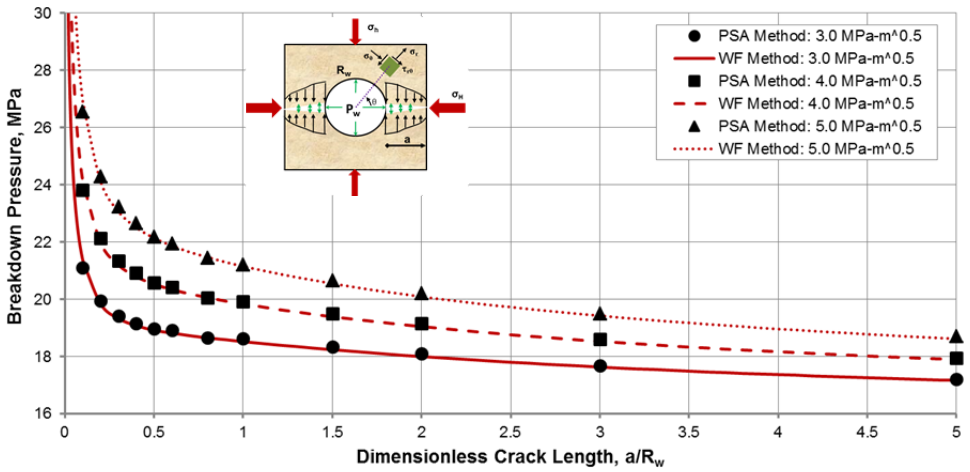

Figure 5 Effect of Fracture Toughness on Breakdown Pressure (R_w = 0.1 m, θ = 0°)

It is observed that (1) the breakdown pressure increases with increasing fracture toughness; (2) breakdown pressures by both methods are in good agreement for different fracture toughnesses; and that (3) the difference in breakdown pressure becomes less with increasing dimensionless crack length. In horizontal well with multi-stage hydraulic fracturing, sometimes the difference in breakdown pressure between stages is attributed to the difference in fracture toughness, if other conditions are the same.

4.5 Influence of Internal Fracture Pressure on Breakdown Pressure

The objective of this paper is not to derive an accurate pressure decline function inside pre-existing fracture, but highlighting the advantages of the weight function method in solving petroleum related fracture mechanics problems. The PSA method is only applicable to the case with constant internal fracture pressure. The weight function method, however, can be applied to study fractures under any nonlinear stress distribution.

The internal pressure distribution for impermeable rock is assumed to be constant, while it is assumed to be a declining function for permeable rock. Assuming that the pressure at the heel of pre-existing fracture is equal to the borehole pressure, and pressure at the tip of the pre-existing fracture is zero because of the existing fluid lag [*Jeffrey*, 1989]. Therefore, the nonlinear fracture pressure distribution is assumed as follows:

$$P(x,R_w)=P_w\left(1-\frac{x^2}{a^2}\right) \tag{15}$$

Keeping all parameters in **Table 2** constant, two cases are investigated: Case I: pressure declines as Eq. 15; Case II: internal pressure is constant, equal to the borehole pressure. The results are depicted in **Fig. 6**. It is observed that breakdown pressure by declining pressure function is about twice that of constant internal pressure of fracture. This emphasizes that the determination of internal pressure distribution function is critical in the calculation of an accurate breakdown pressure.

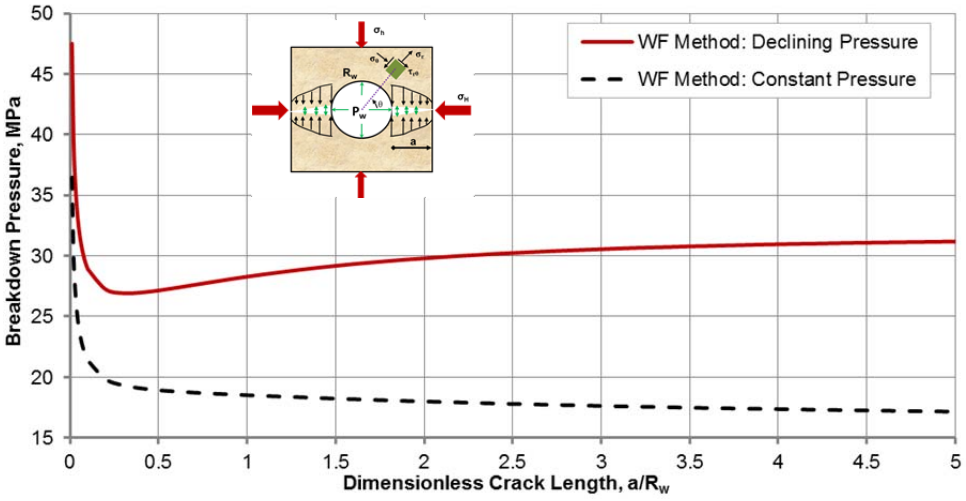

Figure 6 Effect of Pressure Distribution inside Pre-existing Fracture on Breakdown Pressure (R_w = 0.1 m, θ = 0°)

5. Experimental Verification

Scaling laws have been developed for hydraulic fracturing experiments [*De Pater et al.*, 1994; *Berchenko et al.*, 2004]. In this investigation, a triaxial hydraulic fracturing system shown in **Fig. 7** was used to simulate the hydraulic fracturing process in the laboratory. The workflow of the experimental procedure is shown in **Fig. 8**. The properties and dimensions of experimental samples are listed in **Tables 3** and **4**. A high viscosity fracturing fluid was selected to minimize leak-off. The internal pressure distribution is assumed constant. Additional details about the experimental procedures have been published previously [*Zhou et al.*, 2008]. Measured breakdown pressures were selected from experiments conducted for studying fracture propagation, as shown in **Table 5**.

It should be pointed out that many laboratory experiments could not fulfill the research objectives because of the following reasons: the uncertainties of sample properties caused by environment temperature during sample drying (some of the experiments were done in summer, while others were conducted in winter), the difficulty to predict accurate fracture toughness under confining pressure [*Zhao and Roegiers*, 1993], uncemented interface between simulated borehole and sample, complexities in sample preparation and conducting hydraulic fracturing experiments [*Haimson*, 1981]. In addition, the prolonged test and high expenses did not allow the repetitions of all the experiments reported here. Therefore, in order to verify the theoretical breakdown pressures against the measured values, only 6 successful experiments were selected from more than 40 sets of experiments. The experimental conditions and breakdown pressures for these tests are listed in **Table 5**. Fracture toughness for the experimental conditions was not available, so it was fine-tuned to calibrate the theoretical breakdown pressures against the measured values.

The steps of experimental verification are as follows:

Step I: Collect qualified measured breakdown pressures (see **Table 5**).

Step II: Calculate theoretical breakdown pressures with parameters in **Table 5** by fine-tuning fracture toughness at experimental conditions.

Step III: Compare theoretical breakdown pressure against experimental results (see **Fig. 9**).

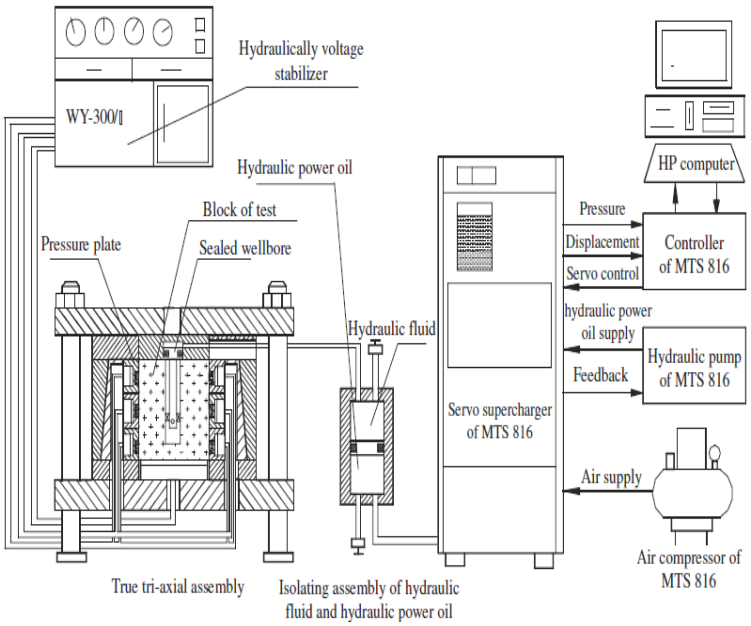

Figure 7 Schematic of Triaxial Hydraulic Fracturing Test System

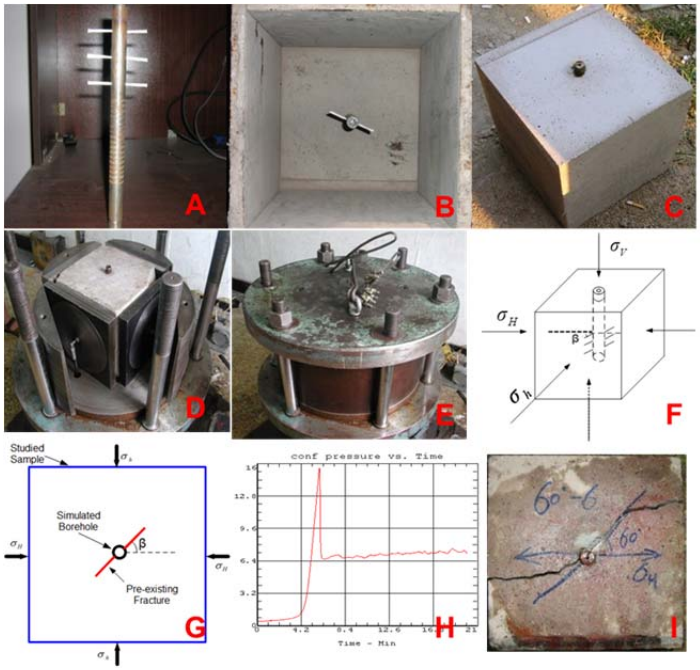

Figure 8 Experiment Setup and Workflow

(A) Simulated borehole with pre-existing fractures radiating from the borehole
(B) Mold of experimental sample. Make samples with different inclination angle by rotating borehole
(C) Sample for hydraulic fracturing test
(D) Sample loading into the cell
(E) Completed assembly
(F) 3-D view of loadings
(G) 2-D view of loadings
(H) Pressure record from the MTS computer system
(I) Fractured sample

Table 3 Physical Properties of Experimental Samples

Parameter	Value
Young's modulus: *E*	15 *GPa*
Poisson's ratio: *v*	0.23
Uniaxial Compressive Strength: *UCS*	48.5 *MPa*
Fracture toughness: K_{IC}	unknown
Permeability: *k*	0.5 md
Porosity: *Ø*	1.85%

Table 4 Dimensions of Experimental Samples

Parameter	Value
Block side length: *L*	0.3 *m*
Borehole radius: R_w	0.1 *m*
Pre-existing Fracture Length: *a*	0.3 *m*

Table 5 Experimental Conditions and Breakdown Pressures[2]

Number[3]	Min In-situ Stress σ_h (*MPa*)	Max In-situ Stress σ_H (*MPa*)	Inclination Angle β °	Measured Breakdown Pressure P_b (*MPa*)
1-4-15	1	4	15	7.4
1-4-30	1	4	30	8.5
1-4-45	1	4	45	9.3
1-4-60	1	4	60	9.8
1-6-30	1	6	30	10.4
1-6-45	1	6	45	10.5
1-6-60	1	6	60	15.6

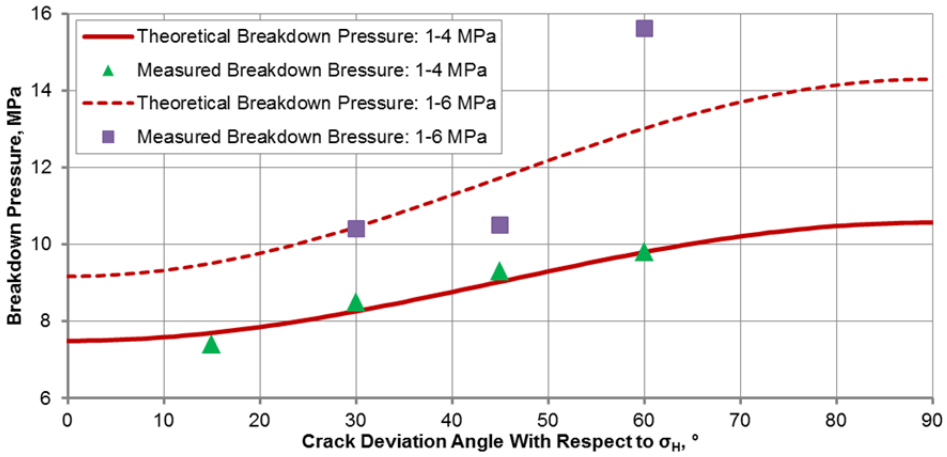

Figure 9 Breakdown Pressure Verification with Experimental Results. The fine-tuned fracture toughness at 1-4 *MPa* is 2.3 *MPa-m*$^{0.5}$, the one at 1-6 *MPa* is 2.9 *MPa-m*$^{0.5}$.

It can be observed from **Fig. 9** that theoretical and experimental breakdown pressures are in good agreement when σ_h = 1 *MPa*, σ_H = 4 *MPa*, but not as good when σ_h = 1 *MPa*, σ_H = 6 *MPa*. The possible reasons for this can be attributed to uncertainty of fracture toughness at high stress contrast and high deviation angle, or that the position of fracture initiation did not takes place at the tip of the pre-existing fracture.

[2] The vertical stress is 15 *MPa*. The high vertical stress was applied to produce plane strain condition.
[3] A-B-C, "A" represents σ_h, "B" represents σ_h, "C" represents deviation angle with respect to σ_H orientation

6. Discussion and Conclusions

We presented the procedure of solving weight function parameters for two pre-existing symmetrical radial cracks emanating from a borehole. A table and three correlation equations of weight function parameters were provided for engineering applications. The weight function method is applied to calculate the breakdown pressure, which is then compared against the breakdown pressure by the PSA method by assuming the internal fracture pressure to be constant. Results of both methods are in very good agreement. This proves the validity of the weight function method in solving for the breakdown pressure. In addition, breakdown pressure by the weight function method was verified against some laboratory hydraulic fracturing experiments. The results were matched by fine-tuning fracture toughness at experimental conditions. Even then, complexities of hydraulic fracturing experiments in some cases lead to disagreement between the experimental and theoretical breakdown pressures.

Sensitivity analyses were conducted to investigate the influence of pre-existing crack length and orientation, fracture toughness, in-situ stress contrast, and internal pressure distribution on breakdown pressure. It is concluded that: (1) breakdown pressure does not always decrease with increasing fracture length; at a relatively large in-situ stress contrast, there is an optimum distance from the borehole wall for a minimum breakdown pressure; (2) breakdown pressure is highly sensitive to a short dimensionless crack length; (3) breakdown pressure changes sinusoidally with the pre-existing crack deviation angle; (4) increasing fracture toughness will increase breakdown pressure, the difference in breakdown pressure, however, becomes less as dimensionless crack length increases; (5) breakdown pressure for the case with nonlinear pressure distribution inside fracture is approximately twice that of constant internal pressure distribution.

The internal pressure distribution (Eq. 15) of pre-existing fracture in this paper was only used to show the difference in breakdown pressures for constant and nonconstant internal pressure distributions. To improve the accuracy of breakdown pressure prediction, one needs to develop a detailed internal pressure function with the inclusion of flow rate, viscosity, borehole pressure, pre-existing length and orientation, etc. In reality, other types of nonlinear stresses, such as thermal stress, chemical stress, if they exist, should also be included in a weight function for calculating *SIFs* under these conditions. The PSA method, however, cannot account for these nonlinear stresses in calculating *SIF*.

This paper covered only weight functions for two symmetrical radial cracks emanating from the borehole. One needs to develop new weight functions for other types of cracks emanating from the borehole. For example, there might be a single, or multiple fractures emanating from the borehole. The weight functions developed in this paper are the same for both deviated and vertical wellbores. The difference in SIFs between vertical and deviated wellbores is caused by different near wellbore stress concentrations.

7. Nomenclature

a = pre-existing fracture depth, *m*

E = Young's modulus for plane stress problem, *GPa*

$f(a/R_w)$ = coefficient for two symmetrical radial cracks from circle

$g(a/R_w)$ = coefficient for two symmetrical radial cracks from circle

k = permeability, *md*

K_I = stress intensity factor of mode I for pre-existing fracture, $MPa\text{-}m^{0.5}$

K_i = stress intensity factor under different net stresses, i = 1, 2, and 3

K_{IC} = fracture toughness of mode I, $MPa\text{-}m^{0.5}$

L = block side length, *cm*

$m(x, a)$ = weight function

M_1, M_2, M_3 = weight function parameters

$P(x, P_w)$ = internal pressure distribution of pre-existing fracture, *MPa*

P_b = breakdown pressure, *MPa*

p_o = pore pressure, *MPa*

P_w = Wellbore pressure, *MPa*

R_w = borehole radius, *m*

T = tensile strength, MPa

UCS = Uniaxial Compressive Strength, *MPa*

x = distance from the borehole wall

Greek letters

β = inclination angle between crack axis and maximum principal stress

$\emptyset$ = Porosity

η = poroelastic constant, *0 – 0.5*

θ = pre-existing crack orientation refer to maximum principal horizontal stress direction, °

υ = Poisson's ratio

σ_H = maximum in-situ stress, *MPa*

σ_h = minimum in-situ stress, *MPa*

Acknowledgement – The authors would like to acknowledge the support from the Well Construction Technology Center at the University of Oklahoma, the Major International (Regional) Joint Research Program of National Natural Science Foundation of China (No.51210006), and the National Natural Science Foundation of China (No. 51204195).

8. References

Abou-Sayed, A., C. Brechtel, and R. Clifton (1978), In situ stress determination by hydrofracturing: a fracture mechanics approach, *Journal of Geophysical Research*, *83*(B6), 2851-2862.

Al-Shayea, N., K. Khan, and S. Abduljauwad (2000), Effects of confining pressure and temperature on mixed-mode (I–II) fracture toughness of a limestone rock, *International Journal of Rock Mechanics and Mining Sciences*, *37*(4), 629-643.

Anderson, T. L. (2005), *Fracture mechanics: fundamentals and applications*, CRC Press.

Atkinson, B. K. (1987), Fracture mechanics approach to hydraulic fracturing stress measurements, in *Fracture mechanics of rocks*, edited, pp. 217-239, Academic Press.

Barry, N., N. R. Whittaker, and S. G. Singh (1992), *Rock fracture mechanics principles design and applications*, ELSEVIER, Amsterdam-London-New York-Tokyo.

Berchenko, I., E. Detournay, N. Chandler, and J. Martino (2004), An in-situ thermo-hydraulic experiment in a saturated granite I: design and results, *International Journal of Rock Mechanics and Mining Sciences*, *41*(8), 1377-1394.

Bueckner, H. (1970), Novel principle for the computation of stress intensity factors, *Zeitschrift fuer Angewandte Mathematik & Mechanik*, *50*(9).

Bunger, A., A. Lakirouhani, and E. Detournay (2010), Modelling the effect of injection system compressibility and viscous fluid flow on hydraulic fracture breakdown pressure, paper presented at Proceedings 5th International Symposium on In-situ Rock Stress, Beijing, China, August 25 - 27, 2010.

De Pater, C., M. Cleary, T. Quinn, D. Barr, D. Johnson, and L. Weijers (1994), Experimental verification of dimensional analysis for hydraulic fracturing, *SPE Production & Facilities*, *9*(4), 230-238.

Detournay, E., and A. Cheng (1992), Influence of pressurization rate on the magnitude of the breakdown pressure, paper presented at Proc. 33nd US Rock Mechanics Symposium, Balkema, Santa Fe, NM, June 3 - 5, 1992.

Detournay, E., and R. Carbonell (1997), Fracture-mechanics analysis of the breakdown process in minifracture or leakoff Test, *Old Production & Facilities*, *12*(3), 195-199.

Dusterhoft, R. (1994), *FracPac completion services-stimulation and sand-control techniques for high-permeability oil and gas wells*, Halliburton Energy Services, Houston.

Economides, M. J., and K. G. Nolte (2000), *Reservoir stimulation*, 3rd ed., Wiley, New York, NY

Fett, T., C. Mattheck, and D. Munz (1987), On the calculation of crack opening displacement from the stress intensity factor, *Engineering Fracture Mechanics*, *27*(6), 697-715.

Fjar, E., R. M. Holt, A. Raaen, R. Risnes, and P. Horsrud (2008), *Petroleum related rock mechanics*, 2nd ed., Elsevier Science.

Glinka, G. (1996), Development of weight functions and computer integration procedures for calculating stress intensity factors around cracks subjected to complex stress fields, *Rep.*, SaFFD, Inc, Petersburg Ontario, Canada.

Glinka, G., and G. Shen (1991), Universal features of weight functions for cracks in mode I, *Engineering Fracture Mechanics*, *40*(6), 1135-1146.

Haimson, B. C. (1981), Large scale laboratory testing of hydraulic fracturing, *Geophysical Research Letters*, *8*(7), 715-718.

Haimson, B. C., and C. Fairhurst (1967), Initiation and extension of hydraulic fractures in rocks, *Old SPE Journal*, *7*(3), 310-318.

Haiqing, W., A.-A. Menahi, H. Ammar, A. Meshary, Q. Moinuddin, and L. Anthony (2004), Image enhancement, automated interpretation, and 3D visualization of borehole image logs in characterization and calibration of fractures in Kuwait, paper presented at Abu Dhabi International Conference and Exhibition, Abu Dhabi, United Arab Emirates, October 10-13, 2004.

Higgins, S. (2006), Geomechanical modeling as a reservoir characterization tool at Rulison, FieldPiceance Basin, Colorado, Master thesis, Colorado School of Mines, Golden, Colorado, USA.

Hubbert, M. K., and D. G. Willis (1957), Mechanics of hydraulic fracturing, *US Geological Survey*, *210*, 153-168.

Ingraffea, A. R. (1977), Discrete fracture propagation in rock: laboratory tests and finite element, Doctoral thesis, University of Colorado, Denver, Colorado.

Ishijima, Y., and J. Roegiers (1983), Fracture initiation and breakdow pressure-Are they similar?, paper presented at the 24th US Symposium on Rock Mechanics (USRMS), College Station, TX, June 20 - 23, 1983.

Jaeger, J. C., and N. G. W. Cook (2007), *Fundamentals of rock mechanics*, 4th ed., Malden, MA, USA.

Jeffrey, R. (1989), The combined effect of fluid lag and fracture toughness on hydraulic fracture propagation, paper presented at the Low Permeability Reservoirs Symposium, Denver, Colorado, March 6-8, 1989.

Jin, X. (2013), Advanced study of hydraulic fracturing, Doctoral thesis, University of Oklahoma, Norman, Oklahoma.

Kiciak, A., G. Glinka, and D. Burns (2003), Calculation of stress intensity factors and crack opening displacements for cracks subjected to complex stress fields, *Journal of pressure vessel technology*, *125*(3), 260-266.

Lord, D., and S. Shah (1994), Study of perforation friction pressure employing a large-scale fracturing flow simulator, paper presented at the SPE Annual Technical Conference and Exhibition, New Orleans, Louisiana, September 25-28, 1994.

Newman Jr, J. (1971), *An improved method of collocation for the stress analysis of cracked plates with various shaped boundaries*, National Aeronautics and Space Administration.

Paris, P. C., and G. C. Sih (1965), Stress analysis of cracks, *ASTM stp*, *381*, 30-83.

Rice, J. R. (1968a), Mathematical analysis in the mechanics of fracture, *Fracture: An advanced treatise*, *2*, 191-311.

Rice, J. R. (1968b), A path independent integral and the approximate analysis of strain concentration by notches and cracks, *Journal of Applied Mechanics*, *35*, 379-386.

Rice, J. R. (1972), Some remarks on elastic crack-tip stress fields, *International Journal of Solids and Structures*, *8*(6), 751-758.

Rummel, F. (1987), Fracture mechanics approach to hydraulic fracturing stress measurements, *Fracture Mechanics of rocks*, 217-240.

Rummel, F., and J. Hansen (1989), Interpretation of hydrofrac pressure recordings using a simple fracture mechanics simulation model, *International Journal of Rock Mechanics and Mining Sciences & Geomechanics Abstracts*, *26*(6), 483-488.

Shen, G., and G. Glinka (1991), Determination of weight functions from reference stress intensity factors, *Theoretical and applied fracture mechanics*, *15*(3), 237-245.

Shlyapobersky, J., G. Wong, and W. Walhaug (1988), Overpressure calibrated design of hydraulic fracture stimulations, paper presented at SPE Annual Technical Conference and Exhibition, Houston, Texas, October 2-5 1988.

Tada, H., P. C. Paris, G. R. Irwin, and H. Tada (2000), *The stress analysis of cracks handbook*, ASME press New York.

Wang, Y., and M. B. Dusseault (1991), Hydraulic fracture stress measurement in rocks with stress-dependent Young's modulus, paper presented at the 32nd US Symposium on Rock Mechanics (USRMS), Norman, Oklahoma, July 10 - 12, 1991.

Weijers, L., C. de Pater, and J. Hagoort (1996), A new mechanism for hydraulic fracture initiation, paper presented at the 2nd North American Rock Mechanics Symposium, Montreal, Quebec, Canada, June 19 - 21, 1996.

Yew, C. H. (1997), *Mechanics of hydraulic fracturing*, 1st ed., Gulf Professional Publishing.

Zhao, X., and J.-C. Roegiers (1993), Determination of in situ fracture toughness, *International journal of rock mechanics and mining sciences & geomechanics abstracts*, *30*(7), 837-840.

Zheng, X., and G. Glinka (1995), Weight functions and stress intensity factors for longitudinal semi-elliptical cracks in thick-wall cylinders, *Journal of pressure vessel technology*, *117*(4), 383-389.

Zheng, X., A. Kiciak, and G. Glinka (1997), Weight functions and stress intensity factors for internal surface semi-elliptical crack in thick-walled cylinder, *Engineering Fracture Mechanics*, *58*(3), 207-221.

Zhou, J., M. Chen, Y. Jin, and G. Zhang (2008), Analysis of fracture propagation behavior and fracture geometry using a tri-axial fracturing system in naturally fractured reservoirs, *International Journal of Rock Mechanics and Mining Sciences*, *45*(7), 1143-1152.

Appendix: Weight function parameters for two symmetrical radial cracks

Table 6 Parameters of weight function for different ratio of crack length to circular radius [*Jin*, 2013].

a/R_w	M_1	M_2	M_3	a/R_w	M_1	M_2	M_3	a/R_w	M_1	M_2	M_3
0.001	-8.5085	9.54248	5.27124	0.36	-0.24015	0.198545	0.599272	2.00	-0.20741	0.059727	0.529864
0.002	-3.8161	4.422013	2.711007	0.37	-0.24951	0.204179	0.60209	2.05	-0.20121	0.054455	0.527228
0.003	-2.2565	2.719114	1.859557	0.38	-0.25836	0.20942	0.60471	2.10	-0.19518	0.049372	0.524686
0.004	-1.4801	1.870579	1.43529	0.39	-0.26673	0.214286	0.607143	2.15	-0.18932	0.044471	0.522235
0.005	-1.0169	1.36377	1.181885	0.40	-0.27465	0.218797	0.609398	2.20	-0.18362	0.039745	0.519873
0.006	-0.7103	1.027805	1.013903	0.41	-0.28212	0.222969	0.611484	2.25	-0.17808	0.035189	0.517595
0.007	-0.4932	0.789452	0.894726	0.42	-0.28918	0.226819	0.613409	2.30	-0.1727	0.030796	0.515398
0.008	-0.332	0.612093	0.806046	0.43	-0.29584	0.230363	0.615182	2.35	-0.16747	0.02656	0.51328
0.009	-0.2081	0.475385	0.737693	0.44	-0.30212	0.233617	0.616808	2.40	-0.16239	0.022474	0.511237
0.01	-0.1102	0.367123	0.683562	0.45	-0.30803	0.236594	0.618297	2.45	-0.15745	0.018533	0.509266
0.02	0.29602	-0.090763	0.454619	0.46	-0.3136	0.239309	0.619655	2.50	-0.15266	0.014731	0.507365
0.03	0.39232	-0.21007	0.394965	0.47	-0.31883	0.241775	0.620887	2.55	-0.148	0.011062	0.505531
0.04	0.41345	-0.246926	0.376537	0.48	-0.32374	0.244003	0.622002	2.60	-0.14347	0.007522	0.503761
0.05	0.40624	-0.252414	0.373793	0.49	-0.32834	0.246007	0.623003	2.65	-0.13907	0.004105	0.502053
0.06	0.38618	-0.243455	0.378273	0.50	-0.33266	0.247797	0.623898	2.70	-0.1348	0.000807	0.500403
0.07	0.35982	-0.227214	0.386393	0.55	-0.35031	0.253897	0.626949	2.75	-0.13065	-0.00238	0.498811
0.08	0.33038	-0.207208	0.396396	0.60	-0.36238	0.256063	0.628032	2.80	-0.12661	-0.00545	0.497273
0.09	0.29959	-0.185334	0.407333	0.65	-0.37001	0.255207	0.627604	2.85	-0.12269	-0.00843	0.495787
0.10	0.26843	-0.162683	0.418658	0.70	-0.3741	0.252044	0.626022	2.90	-0.11888	-0.0113	0.494352
0.11	0.2375	-0.139913	0.430043	0.75	-0.37536	0.247133	0.623567	2.95	-0.11517	-0.01407	0.492965
0.12	0.20717	-0.117429	0.441285	0.80	-0.37437	0.240916	0.620458	3.00	-0.11157	-0.01675	0.491624
0.13	0.17764	-0.095484	0.452258	0.85	-0.37161	0.233737	0.616869	3.05	-0.10807	-0.01934	0.490328
0.14	0.14906	-0.074236	0.462882	0.90	-0.36745	0.22587	0.612935	3.10	-0.10466	-0.02185	0.489074
0.15	0.12151	-0.05378	0.47311	0.95	-0.3622	0.217529	0.608765	3.15	-0.10135	-0.02428	0.487862
0.16	0.09502	-0.03417	0.482915	1.00	-0.3561	0.208882	0.604441	3.20	-0.09812	-0.02662	0.486689
0.17	0.06961	-0.015432	0.492284	1.05	-0.34935	0.200062	0.600031	3.25	-0.09499	-0.02889	0.485554
0.18	0.04528	0.002427	0.501214	1.10	-0.34212	0.191171	0.595585	3.30	-0.09193	-0.03109	0.484456
0.19	0.02201	0.019413	0.509706	1.15	-0.33454	0.18229	0.591145	3.35	-0.08896	-0.03321	0.483393
0.20	-0.0002	0.035539	0.51777	1.20	-0.32672	0.173483	0.586741	3.40	-0.08607	-0.03527	0.482363
0.21	-0.0214	0.050828	0.525414	1.25	-0.31874	0.164796	0.582398	3.45	-0.08325	-0.03727	0.481366
0.22	-0.0417	0.065303	0.532652	1.30	-0.31068	0.156265	0.578133	3.50	-0.08051	-0.0392	0.4804
0.23	-0.0609	0.078993	0.539496	1.35	-0.30259	0.147919	0.57396	3.55	-0.07784	-0.04107	0.479464
0.24	-0.0793	0.091925	0.545962	1.40	-0.29453	0.139776	0.569888	3.60	-0.07524	-0.04288	0.478558
0.25	-0.0968	0.10413	0.552065	1.45	-0.28652	0.131851	0.565926	3.65	-0.0727	-0.04464	0.477679
0.26	-0.1134	0.115637	0.557818	1.50	-0.2786	0.124152	0.562076	3.70	-0.07024	-0.04635	0.476826
0.27	-0.1292	0.126476	0.563238	1.55	-0.27079	0.116685	0.558342	3.75	-0.06783	-0.048	0.476
0.28	-0.1443	0.136677	0.568338	1.60	-0.26311	0.109451	0.554726	3.80	-0.06548	-0.0496	0.475199
0.29	-0.1586	0.146268	0.573134	1.65	-0.25557	0.102452	0.551226	3.85	-0.06319	-0.05116	0.474421
0.30	-0.1721	0.155276	0.577638	1.70	-0.24819	0.095685	0.547843	3.90	-0.06096	-0.05267	0.473667
0.31	-0.185	0.163729	0.581865	1.75	-0.24097	0.089148	0.544574	3.95	-0.05879	-0.05413	0.472935
0.32	-0.1972	0.171654	0.585827	1.80	-0.23391	0.082835	0.541418	4.00	-0.05667	-0.05555	0.472224
0.33	-0.2088	0.179074	0.589537	1.85	-0.22703	0.076743	0.538371	4.05	-0.0546	-0.05693	0.471535
0.34	-0.2198	0.186014	0.593007	1.90	-0.22032	0.070865	0.535432	4.10	-0.05258	-0.05827	0.470865
0.35	-0.2303	0.192497	0.596248	1.95	-0.21378	0.065195	0.532598	4.15	-0.05061	-0.05957	0.470214

a/R_w	M_1	M_2	M_3	a/R_w	M_1	M_2	M_3	a/R_w	M_1	M_2	M_3
4.20	-0.0487	-0.060835	0.469582	6.60	0.00778	-0.09456	0.452721	9.00	0.031133	-0.10554	0.447228
4.25	-0.0468	-0.062063	0.468968	6.65	0.008478	-0.09492	0.452539	9.05	0.031461	-0.10568	0.447161
4.30	-0.045	-0.063256	0.468372	6.70	0.009164	-0.09528	0.452361	9.10	0.031784	-0.10581	0.447097
4.35	-0.0432	-0.064416	0.467792	6.75	0.009838	-0.09563	0.452187	9.15	0.032102	-0.10593	0.447033
4.40	-0.0414	-0.065543	0.467228	6.80	0.010501	-0.09597	0.452017	9.20	0.032416	-0.10606	0.446971
4.45	-0.0397	-0.066639	0.46668	6.85	0.011152	-0.0963	0.45185	9.25	0.032726	-0.10618	0.44691
4.50	-0.038	-0.067705	0.466148	6.90	0.011791	-0.09662	0.451688	9.30	0.033032	-0.1063	0.44685
4.55	-0.0364	-0.068741	0.46563	6.95	0.01242	-0.09694	0.451529	9.35	0.033333	-0.10642	0.446792
4.60	-0.0348	-0.069749	0.465125	7.00	0.013038	-0.09725	0.451373	9.40	0.03363	-0.10653	0.446734
4.65	-0.0333	-0.07073	0.464635	7.05	0.013646	-0.09756	0.451221	9.45	0.033924	-0.10664	0.446678
4.70	-0.0317	-0.071684	0.464158	7.10	0.014243	-0.09786	0.451072	9.50	0.034213	-0.10675	0.446623
4.75	-0.0303	-0.072613	0.463694	7.15	0.014831	-0.09815	0.450926	9.55	0.034499	-0.10686	0.446568
4.80	-0.0288	-0.073517	0.463242	7.20	0.015408	-0.09843	0.450784	9.60	0.03478	-0.10697	0.446515
4.85	-0.0274	-0.074397	0.462802	7.25	0.015976	-0.09871	0.450644	9.65	0.035058	-0.10707	0.446463
4.90	-0.026	-0.075253	0.462373	7.30	0.016535	-0.09898	0.450508	9.70	0.035332	-0.10718	0.446412
4.95	-0.0246	-0.076088	0.461956	7.35	0.017085	-0.09925	0.450374	9.75	0.035603	-0.10728	0.446362
5.00	-0.0233	-0.0769	0.46155	7.40	0.017625	-0.09951	0.450243	9.80	0.03587	-0.10737	0.446313
5.05	-0.022	-0.077692	0.461154	7.45	0.018157	-0.09977	0.450115	9.85	0.036134	-0.10747	0.446265
5.10	-0.0207	-0.078463	0.460769	7.50	0.01868	-0.10002	0.44999	9.90	0.036394	-0.10756	0.446218
5.15	-0.0194	-0.079214	0.460393	7.55	0.019195	-0.10026	0.449868	9.95	0.036651	-0.10766	0.446172
5.20	-0.0182	-0.079946	0.460027	7.60	0.019701	-0.1005	0.449748	10	0.036904	-0.10775	0.446126
5.25	-0.017	-0.080659	0.45967	7.65	0.0202	-0.10074	0.44963	11	0.041354	-0.10923	0.445385
5.30	-0.0158	-0.081355	0.459323	7.70	0.02069	-0.10097	0.449515	12	0.044851	-0.11022	0.444888
5.35	-0.0147	-0.082033	0.458984	7.75	0.021173	-0.1012	0.449402	13	0.047643	-0.11088	0.44456
5.40	-0.0136	-0.082694	0.458653	7.80	0.021648	-0.10142	0.449292	14	0.049905	-0.1113	0.444351
5.45	-0.0125	-0.083338	0.458331	7.85	0.022116	-0.10163	0.449184	15	0.051759	-0.11154	0.444228
5.50	-0.0114	-0.083967	0.458017	7.90	0.022577	-0.10184	0.449079	16	0.053295	-0.11167	0.444166
5.55	-0.0103	-0.08458	0.45771	7.95	0.02303	-0.10205	0.448975	17	0.054579	-0.1117	0.444149
5.60	-0.0093	-0.085178	0.457411	8.00	0.023476	-0.10225	0.448874	18	0.055661	-0.11167	0.444165
5.65	-0.0083	-0.085761	0.457119	8.05	0.023916	-0.10245	0.448774	19	0.056581	-0.11159	0.444206
5.70	-0.0073	-0.086331	0.456835	8.10	0.024349	-0.10265	0.448677	20	0.057366	-0.11147	0.444264
5.75	-0.0063	-0.086886	0.456557	8.15	0.024775	-0.10284	0.448582	25	0.05996	-0.11063	0.444687
5.80	-0.0053	-0.087428	0.456286	8.20	0.025195	-0.10302	0.448488	30	0.061304	-0.10967	0.445167
5.85	-0.0044	-0.087957	0.456021	8.25	0.025609	-0.10321	0.448397	35	0.062048	-0.10876	0.44562
5.90	-0.0035	-0.088474	0.455763	8.30	0.026016	-0.10339	0.448307	40	0.062474	-0.10795	0.446027
5.95	-0.0026	-0.088978	0.455511	8.35	0.026418	-0.10356	0.44822	45	0.06272	-0.10723	0.446387
6.00	-0.0017	-0.08947	0.455265	8.40	0.026813	-0.10373	0.448134	50	0.062857	-0.10659	0.446705
6.05	-0.0008	-0.089951	0.455025	8.45	0.027202	-0.1039	0.448049	55	0.062928	-0.10603	0.446987
6.10	5.2E-05	-0.09042	0.45479	8.50	0.027586	-0.10407	0.447967	60	0.062956	-0.10553	0.447237
6.15	0.00089	-0.090879	0.454561	8.55	0.027965	-0.10423	0.447886	65	0.062956	-0.10508	0.447461
6.20	0.00171	-0.091327	0.454337	8.60	0.028337	-0.10439	0.447807	70	0.062938	-0.10468	0.447662
6.25	0.00252	-0.091764	0.454118	8.65	0.028705	-0.10454	0.447729	75	0.062908	-0.10431	0.447844
6.30	0.00331	-0.092192	0.453904	8.70	0.029067	-0.10469	0.447653	80	0.062871	-0.10398	0.448008
6.35	0.00409	-0.092609	0.453695	8.75	0.029423	-0.10484	0.447579	85	0.062829	-0.10368	0.448159
6.40	0.00486	-0.093017	0.453491	8.80	0.029775	-0.10499	0.447506	90	0.062784	-0.10341	0.448296
6.45	0.00561	-0.093416	0.453292	8.85	0.030122	-0.10513	0.447434	95	0.062737	-0.10316	0.448422
6.50	0.00634	-0.093806	0.453097	8.90	0.030464	-0.10527	0.447364	100	0.062689	-0.10292	0.448539
6.55	0.00707	-0.094186	0.452907	8.95	0.030801	-0.10541	0.447295				